Applied Physics Express 4 (2011) 092103
DOI: 10.1143/APEX.4.092103

# GaN-Based Light-Emitting Diodes Grown on Nanoscale Patterned Sapphire Substrates with Void-Embedded Cortex-Like Nanostructures

Yu-Sheng Lin[1] and J. Andrew Yeh[1,2,3]*

[1]*Institute of NanoEngineering and MicroSystems, National Tsing Hua University, Hsinchu 30013, Taiwan, R.O.C.*
[2]*Instrument Technology Research Center (ITRC), National Applied Research Laboratories, Hsinchu 300, Taiwan, R.O.C.*
[3]*Department of Power Mechanical Engineering, National Tsing Hua University, Hsinchu 30013, Taiwan, R.O.C.*

Received June 21, 2011; accepted August 6, 2011; published online August 25, 2011

High-efficiency GaN-based light-emitting diodes (LEDs) with an emitting wavelength of 438 nm were demonstrated utilizing nanoscale patterned sapphire substrates with void-embedded cortex-like nanostructures (NPSS-VECN). Unlike the previous nanopatterned sapphire substrates, the presented substrate has a new morphology that can not only improve the crystalline quality of GaN epilayers but also generate a void-embedded nanostructural layer to enhance light extraction. Under a driving current of 20 mA, the external quantum efficiency of an LED with NPSS-VECN is enhanced by 2.4-fold compared with that of the conventional LED. Moreover, the output powers of two devices respectively are 33.1 and 13.9 mW. 

GaN-based light-emitting diodes (LEDs) are the most promising solid-state light sources for lighting, full color displays, traffic signals, automobile headlights, etc. Although GaN-based LEDs are commercially available, it is still necessary to further improve the internal quantum efficiency (IQE) and light extraction efficiency (LEE) to increase the performance of light output. The performance of GaN-based LEDs is affected dramatically by inherent threading dislocations (TDs) in the epilayers resulting from the mismatch of lattice constants and thermal expansion coefficients between heterolayers. The TDs will reduce the IQE by providing a leakage pathway for electron–hole pairs to pass through the active regions.[1)] The high refractive index of GaN ($n_{GaN} = 2.45$) constrains light within a critical angle from being extracted because of the different refraction indices of GaN and air. To minimize TD density, nanoscale epitaxial lateral overgrowth[2)] and nanoscale patterned sapphire substrates (NPSS) were proposed.[3–9)] Patterned sapphire substrates,[10)] photonic crystal structures,[11,12)] periodic deflector embedded structures,[13)] an omnidirectional reflector on the backside of the sapphire substrate,[14)] and the lift-off process[15,16)] have been used to increase the LEE in GaN-based LEDs on sapphire substrates. Thus, it is of great interest to improve the IQE while maintaining a high LEE by using a NPSS technique for high-efficiency LEDs.

The morphology of the NPSS, as reported in the literature, includes periodic nanolenses,[3–5)] nanopillars,[6)] nanoholes,[7)] and aperiodic nanopillars.[8,9)] The epitaxial crystalline quality on the NPSS with a nanolens array can be improved owing to the dislocation bending in the GaN epilayer.[4)] Such a morphology cannot construct the void-embedded nanostructural layer at the GaN/sapphire interface owing to the GaN epilayer filled with the depressions between nanolenses without epitaxial lateral overgrowth. The NPSS with the periodic nanopillars and nanoholes can improve the IQE and LEE at the same time.[6,7)] The common feature of these morphologies is that no *c*-facet sapphire exists on the depressions, which resulted in the *c*-plane GaN starting to grow on the *c*-plane terraces of the NPSS, and then extending and coalescing atop the NPSS. Thus, the periodic morphologies induce the formation of void-embedded nanostructural layer between the GaN and sapphire substrates, which allows the light to reflect back to the device by the different refraction indices of GaN and NPSS. As for the morphology of the NPSS with aperiodic nanopillars, the nanostructures were distributed randomly over a large-scale area having few voids embedded between GaN and sapphire with a limited increase in LEE.[8,9)]

In this paper, we present a new morphology of the NPSS with void-embedded cortex-like nanostructures (NPSS-VECN) patterned by natural lithography, which has substantially different nanostructures from those reported in the literature. The GaN epilayer does not easily fill the depressions owing to there being no *c*-facet sapphire exposed between cortex-like nanostructures. Such a morphology cannot only promote the *c*-plane GaN lateral overgrowth but also construct the VECN at the GaN/sapphire interface, and then enhance the external quantum efficiency (EQE) of LEDs. The diverse nanostructures with exposed *c*-plane terraces were distributed uniformly over a large-scale area by inductively coupled plasma etching of a textured thin film. Furthermore, the LED structures fabricated on an NPSS with void-embedded cortex-like nanostructures (LED-VECN) exhibited higher light output power than that fabricated on conventional sapphire substrates (LED-CSS). The comparison of geometric morphologies and optoelectronic properties between the LED-VECN and LED-CSS is carried out in detail.

Two-inch single-side-polished (0001) *c*-plane sapphire wafers of 430 μm thickness were used to fabricate the NPSS-VECN. The flow began with a layer of 2-μm-thick polysilicon deposited by low-pressure chemical vapor deposition at 640 °C. Next, the substrate was dipped in diluted Wright etching solution[17)] [mixed acid solution : deionized (DI) water = 1 : 5] for 30 min to texture the thin-film surface. Thus, the textured nanostructures were formed to be a hard mask for subsequent etching of the sapphire substrate. The wafer was vertically etched using inductively coupled plasma-reactive ion etching (ICP-RIE) with a $BCl_3/Cl_2$ mixed gas at 90 sccm, 5 mTorr, and a source power of 1900 W for 10 min. Finally, the hard mask was removed by a hot KOH solution at 80 °C. The morphology of the NPSS-VECN was characterized by atomic force microscopy (AFM), as shown in Fig. 1(a), revealing the nanostructures of 50–150 nm in spacing, 80–150 nm in depth, and $10^{10}$ $cm^{-2}$ in density. The LED structures were then grown by low-pressure metal–organic chemical vapor deposition (MOCVD) with a rotating-disk reactor. A 30-nm-thick GaN nucleation layer

*E-mail address: jayeh@mx.nthu.edu.tw

 

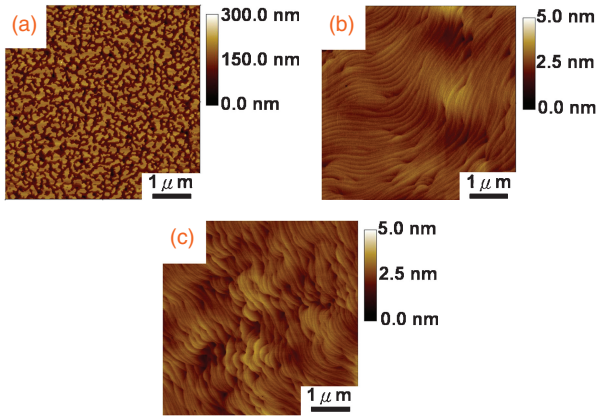


**Fig. 1.** AFM images of (a) NPSS-VECN, (b) u-GaN-VECN, and (c) u-GaN-CSS. The scan area is $5 \times 5\,\mu m^2$.

and a 2.5-μm-thick undoped GaN (u-GaN) buffer layer were sequentially grown at 530 and 1050 °C by MOCVD. The root-mean-square surface roughness for u-GaN of 0.3 nm was observed by AFM over the scan area of $5 \times 5\,\mu m^2$, as shown in Fig. 1(b). The pit density is in the range of $10^7$–$10^8\,cm^{-2}$ for u-GaN grown on NPSS-VECN (u-GaN-VECN), smaller than that grown on CSS (u-GaN-CSS) by two orders [$10^9$–$10^{10}\,cm^{-2}$, as shown in Fig. 1(c)]. These pits were produced by the TDs propagating to the top surface of GaN, which originates from the underlying GaN/sapphire interface. The formation of pits could be induced due to insufficient energy of Ga atoms to migrate to proper sites.[18,19] Figure 2(a) shows the crystalline quality of the u-GaN samples examined by double-crystal X-ray diffraction (XRD). The full-widths at half maximum (FWHM) of the (0002) X-ray rocking curves of u-GaN-VECN and u-GaN-CSS were found to be 211 and 294 arcsec, respectively. The results indicated that the crystalline quality of the GaN epilayer was effectively improved by using the NPSS-VECN technique.

The LED structures were composed of a 2-μm-thick Si-doped GaN layer (n-GaN), an unintentionally doped active region with five periods of InGaN/GaN multiple quantum wells (MQWs), 30-nm-thick Mg-doped AlGaN/GaN superlattices as the electron blocking layer, and 100-nm-thick Mg-doped GaN layer (p-GaN). The surface of LEDs was partially etched until the n-GaN layer was exposed. Followed by deposition of indium balls onto the exposed n-GaN and p-GaN layers to serve as the n-type electrode and p-type electrode, respectively without encapsulation. The optoelectronic characteristics were conducted on the bare wafer-level LEDs. The inset of Fig. 2(b) shows a schematic diagram of the LED-VECN. The crystalline quality of the devices was examined by the high-resolution double-crystal XRD of $\omega$–$2\theta$ scans for the (0002) reflections from the LED-VECN and the LED-CSS. The strongest peak in both spectra originates from the u-GaN layers. The FWHMs of X-ray rocking curves for the LED-VECN and the LED-CSS were found to be 216 and 256 arcsec, respectively, which coincided with Fig. 2(a). This confirms that the LED-VECN has better crystalline quality than the LED-CSS.[5] In addition, the well-defined high-order satellite diffraction peaks of up to the fifth order can be distinguished, indicating good layer periodicity and InGaN/GaN interfaces.[20]

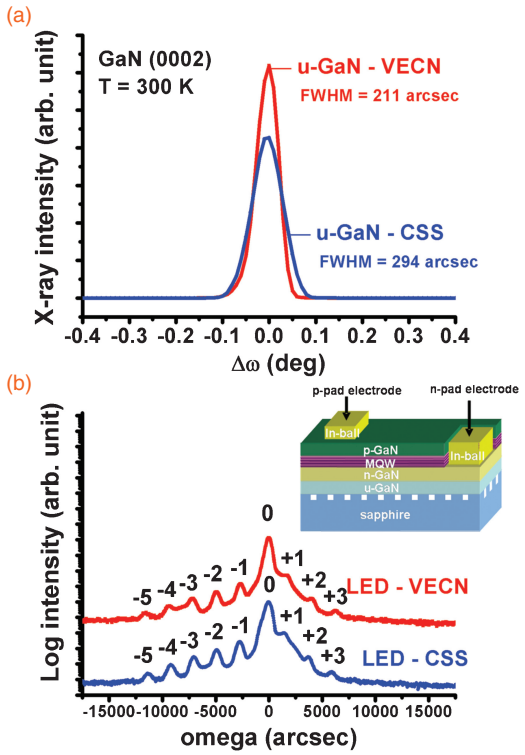


**Fig. 2.** (a) X-ray rocking curves of u-GaN grown on NPSS-VECN and CSS. (b) High-resolution X-ray diffraction of $\omega$–$2\theta$ (0002) scans for the LED-VECN and the LED-CSS. The inset shows a schematic diagram of the LED-VECN.

The optoelectronic characteristics of the LED-VECN and the LED-CSS are compared in Fig. 3, including the electroluminescence (EL), light output power–current–voltage characteristics ($L$–$I$–$V$), and EQE. Figure 3(a) shows the EL spectra of the LED-VECN and the LED-CSS under a driving current of 20 mA at room temperature (300 K). The peak wavelengths of EL spectra were located at 438 nm and the EL intensity of the LED-VECN was increased by 31.3% in comparison with that of the LED-CSS. In Fig. 3(b), the $I$–$V$ curves of the LED-VECN and the LED-CSS measured at room temperature reveal that the forward voltages of the LED-VECN (3.6 V) are smaller than that of LED-CSS (3.8 V) under the same driving current of 20 mA. Figure 3(c) shows the output power of LEDs measured from top of the devices, using an integrating sphere combing with a calibrated power meter and a semiconductor device analyzer. The output power of the LED-VECN was larger than that of the LED-CSS for the driving currents of up to 160 mA. Under an injection current of 20 mA, the output power of the LED-VECN (33.1 mW) was increased 2.4-fold higher than that of the LED-CSS (13.9 mW). Figure 3(d) shows that the corresponding EQEs are 58.3 and 24.5% for the LED-VECN and the LED-CSS at 20 mA, respectively. The EQE value for the LED-VECN is comparable to that on the nanopatterned sapphire substrates, which is 40–50% in the literature.[2,8] Such a significant enhancement in EL intensity and output power could be explained by the following two reasons; improvement of quantum efficiency by reducing the dislocation density, and increased light reflected by the air-void embedded at the GaN/sapphire interface.

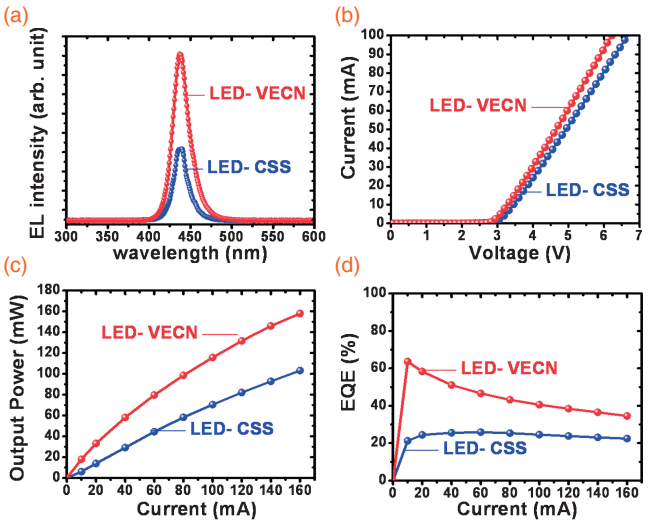


**Fig. 3.** (a) The EL spectra show the emitting wavelength of the LED-VECN and the LED-CSS located at the 438 nm under an injection current of 20 mA. (b) *I–V* curves of the LED-VECN and the LED-CSS, (c) light output power, and (d) EQE in relation to current characteristics of the LED-VECN and the LED-CSS, respectively.

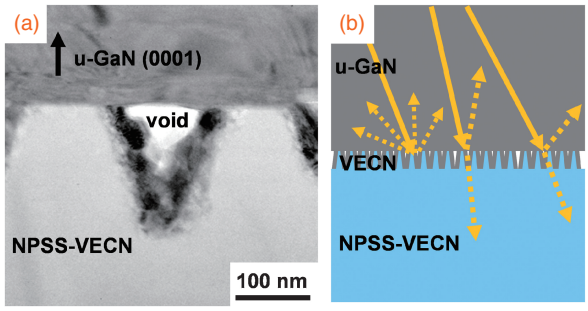


**Fig. 4.** (a) Cross-sectional TEM image and (b) simple optical ray diagram at the u-GaN/NPSS-VECN interface.

Figure 4(a) shows the cross-sectional transmission electron microscopy (TEM) image of the u-GaN/NPSS-VECN interface. Voids were formed beneath the laterally extended and coalesced u-GaN film atop *c*-facet sapphire terraces. No *c*-facets are exposed on sapphire depressions due to the plasma of ICP-RIE damaging the *c*-facets on depressions, which resulted in the *c*-plane GaN starting to grow on the *c*-plane terraces of sapphire, and then extending and coalescing on surface. The spectral reflectance of the u-GaN-VECN and the u-GaN-CSS has been computed by finite-difference time-domain (FDTD) with u-GaN as the incident medium. The results indicated that the high refractive index of the u-GaN ($n_{GaN} = 2.45$) compared with these of the void ($n_{air} = 1$) and sapphire ($n_s = 1.78$) will constrain the light reflected in the top direction between the u-GaN film and the VECN ($1 < n_{VECN} < 1.78$), as shown in Fig. 4(b). The reflectance of LEDs was analyzed using a spectrometer at normal incidence under visible spectrum. The average reflectance of the LED-VECN is 32.8% higher than that of the LED-CSS at 438-nm wavelength. The results indicated that light extraction efficiency can be enhanced by using the NPSS-VECN technique. Larger output powers can be achieved from the LEDs fabricated on the NPSS-VECN.

In this study, the NPSS-VECN was fabricated to effectively improve not only crystalline quality but also light extraction. The measurement results of XRD and AFM infer that the crystalline quality of the LEDs is improved by using the NPSS-VECN technique. Under an injection current of 20 mA, the LED-VECN exhibited 58.3% in EQE, which was increased 2.4-fold higher than that of the LED-CSS. The improvement of the EQE for the LED-VECN is attributed not only to the enhancement of light extraction efficiency via the void-embedded nanostructural layer that efficiently reflected the light back to the device, but also to the reduction of threading dislocations using the NPSS-VECN technique. The method of NPSS-VECN is a cost-effective solution to the wafer-level cortex-like nanostructures on sapphire for high-efficiency LEDs without implementation of an expensive semiconductor mask. These results make it possible to acquire high light output efficiency and it is thought that these developments can provide a candidate method for elevating the emission efficiency of commercial light-emitting devices.

**Acknowledgment** The authors gratefully acknowledge the Sino-American Silicon Products Incorporation and the financial support for this research from the National Science Council of Taiwan under grant No. NSC 98-2622-E-007-011-CC3.

1) S. D. Lester, F. A. Ponce, M. G. Craford, and D. A. Steigerwald: Appl. Phys. Lett. **66** (1995) 1249.
2) C. H. Chiu, H. H. Yen, C. L. Chao, Z. Y. Li, P. Yu, H. C. Kuo, T. C. Lu, S. C. Wang, K. M. Lau, and S. J. Cheng: Appl. Phys. Lett. **93** (2008) 081108.
3) C. C. Kao, Y. K. Su, C. L. Lin, and J. J. Chen: Appl. Phys. Lett. **97** (2010) 023111.
4) H. W. Huang, J. K. Huang, S. Y. Kuo, K. Y. Lee, and H. C. Kuo: Appl. Phys. Lett. **96** (2010) 263115.
5) J. J. Chen, Y. K. Su, C. L. Lin, S. M. Chen, W. L. Li, and C. C. Kao: IEEE Photonics Technol. Lett. **20** (2008) 1193.
6) C. H. Chan, C. H. Hou, S. Z. Tseng, T. J. Chen, H. T. Chien, F. L. Hsiao, C. C. Lee, Y. L. Tsai, and C. C. Chen: Appl. Phys. Lett. **95** (2009) 011110.
7) H. W. Huang, C. H. Lin, J. K. Huang, K. Y. Lee, C. F. Lin, C. C. Yu, J. Y. Tsai, R. Hsueh, H. C. Kuo, and S. C. Wang: Mater. Sci. Eng. B **164** (2009) 76.
8) H. Gao, F. Yan, Y. Zhang, J. Li, Y. Zeng, and G. Wang: J. Appl. Phys. **103** (2008) 014314.
9) H. Gao, F. Yan, Y. Zhang, J. Li, Y. Zeng, and G. Wang: Phys. Status Solidi A **205** (2008) 1719.
10) D. S. Wuu, W. K. Wang, K. S. Wen, S. C. Huang, S. H. Lin, S. Y. Huang, C. F. Lin, and R. H. Horng: Appl. Phys. Lett. **89** (2006) 161105.
11) T. S. Kim, S. M. Kim, Y. H. Jang, and G. Y. Jung: Appl. Phys. Lett. **91** (2007) 171114.
12) D. H. Kim, C. O. Cho, Y. G. Roh, H. Jeon, Y. S. Park, J. Cho, J. S. Im, C. Sone, Y. Park, W. J. Choi, and Q. H. Park: Appl. Phys. Lett. **87** (2005) 203508.
13) H. G. Kim, M. G. Na, H. K. Kim, H. Y. Kim, J. H. Ryu, T. V. Cuong, and C. H. Hong: Appl. Phys. Lett. **90** (2007) 261117.
14) C. H. Lin, H. C. Kuo, C. F. Lai, H. W. Huang, K. M. Leung, C. C. Yu, and J. R. Lo: Semicond. Sci. Technol. **21** (2006) 1513.
15) T. Fujii, Y. Gao, R. Sharma, E. L. Hu, S. P. DenBaars, and S. Nakamura: Appl. Phys. Lett. **84** (2004) 855.
16) C. F. Lin, J. J. Dai, M. S. Lin, K. T. Chen, W. C. Huang, C. M. Lin, R. H. Jiang, and Y. C. Huang: Appl. Phys. Express **3** (2010) 031001.
17) M. W. Jenkins: J. Electrochem. Soc. **124** (1977) 757.
18) D. I. Florescu, S. M. Ting, J. C. Ramer, D. S. Lee, V. N. Merai, A. Parkeh, D. Lu, E. A. Armour, and L. Chernyak: Appl. Phys. Lett. **83** (2003) 33.
19) S. M. Ting, J. C. Ramer, D. I. Florescu, V. N. Merai, B. E. Albert, A. Parkeh, D. S. Lee, D. Lu, D. V. Christini, L. Liu, and E. A. Armour: J. Appl. Phys. **94** (2003) 1461.
20) C. H. Chen, S. J. Chang, Y. K. Su, G. C. Chi, J. K. Sheu, and J. F. Chen: IEEE J. Sel. Top. Quantum Electron. **8** (2002) 284.